Urol Res (1997) 25:59–65

ORIGINAL PAPER

Y. Naito · Y. Ohtawara · S. Kageyama · M. Nakano
A. Ichiyama · M. Fujita · K. Suzuki · K. Kawabe · I. Kino

Morphological analysis of renal cell culture models of calcium phosphate stone formation

Received: 11 October 1995 / Accepted: 18 June 1996

Abstract Cell culture models of calcium phosphate renal stone formation were established using the MDCK cell line. Renal microliths were detected within pseudocysts in three-dimensional soft agar cultures, and were also observed in the basal region of cells lining the cell sheet, and immediately beneath domes or blisters in monolayers and collagen gel cultures. Light and scanning electron microscopy indicated that these microliths had a similar lamellated and spherical appearance to those in humans. These microliths were first detected microscopically after 21 days of culture, and were found to be composed of calcium phosphate by X-ray and micro-infrared spectroscopic analyses. These culture models may provide a powerful new tool to study the pathogenesis of renal stone diseases and/or calcium phosphate stone formation in humans and animals.

Key words Renal stone · Cell culture models · MDCK cell line · Calcium phosphate

Y. Naito, (✉) · I. Kino
First Department of Pathology, Hamamatsu University School of Medicine, 3600 Handa-cho, Hamamatsu 431-31, Japan

Y. Ohtawara · S. Kageyama · M. Nakano · K. Suzuki
Department of Urology, Hamamatsu University School of Medicine, 3600 Handa-cho, Hamamatsu-shi, Shizuoka 431-31, Japan

A. Ichiyama
First Department of Biochemistry, Hamamatsu University School of Medicine, 3600 Handa-cho, Hamamatsu-shi, Shizuoka 431-31, Japan

M. Fujita
Second Department of Biochemistry, Hamamatsu University School of Medicine, 3600 Handa-cho, Hamamatsu-shi, Shizuoka 431-31, Japan

K. Kawabe
Department Urology, Faculty of Medicine, University of Tokyo, 7-3-1 Hongo, Bunkyou-ku, Tokyo 113, Japan

Introduction

Renal lithiasis is a common disease in humans and there have been many reports on the mechanisms of its development [1, 11, 14, 18, 28, 30–32, 37]. Two factors are thought to control renal calculogenesis. Anatomically, impaired drainage from the kidney may reduce the flow of urine, and so increase the risk of retention and aggregation of stone-forming materials in the urinary tract. Physicochemically, crystal aggregates may be formed as the result of an imbalance between the level of inhibitors of crystallization in the urine [7, 17, 27, 34, 42, 43] and the degree of supersaturation of various calculous-forming salts and other lithogenic promoters [3, 15, 28, 33, 35, 45]. Renal lithiasis is also associated with many extraurinary factors, such as age, sex, genetic and dietary factors, and climatic and geographical environments [1, 8, 13, 18, 26, 28, 38, 41]. However, the mechanisms of stone formation are still not fully understood. It is necessary to study the events of renal stone formation more closely at the cellular and molecular level, and to establish links between basic and clinical events in the field.

Cell culture models may enable closer analysis of renal calculogenesis at the cellular and molecular level. Currently, no such models exist, though there have been many reports of renal stone adherent and endocytosis experiments using exogenous calcium oxalate and/or calcium phosphate crystals in cell cultures [20, 21, 23–25, 33, 44], and experimental animal models may in part mimic the etiology of human nephrolithiasis [9, 10, 22]. In the present study, cell culture models of experimental renal calculogenesis were established using an MDCK (Madine Darby Canine Kidney) cell line derived from canine renal distal tubular epithelium [12, 16].

Materials and methods

Cell culture

The MDCK cell line was maintained by serial passage under static culture conditions in Dulbecco's Modified Eagle Medium (Nissui Seiyaku Ltd.) supplemented with 10% fetal bovine serum (Filtron PTY Ltd.) under a 5% CO_2 atmosphere at 37°C. The cells were grown as monolayers in plastic culture flasks, and at confluence they formed "domes" or "blisters" (Fig. 1).

For monolayer culture, MDCK cells were seeded at 5×10^5 cells/60-mm plastic dish (Nunc) and the medium was renewed once every 2 or 3 days. For three-dimensional soft agar culture, 100 cells were embedded in 2 ml 0.33% soft agar medium on a 2 ml 0.5% agar-basal layer (acting as feeder layer) into a 60-mm plastic dish. For collagen gel culture, 5×10^5 cells were plated on the surface of a collagen layer (Kouken Ltd) in a 35-mm plastic dish. One milliliter of culture medium was added every 2 weeks for refeeding and to prevent drying on the surface of soft agar matrix or the collagen layer. The cultivation period of the three types of culture model was up to 60 days without transfer.

Light microscopy

Cultured cells from the three types of culture system were harvested every 5 and/or 7 days and fixed in 10% formalin for 24 h, embedded in paraffin, and sectioned at 3-μm thickness. Paraffin sections were stained with hematoxylin and eosin for morphological examination and by von Kossa's method to detect microliths and calcifications. Colony efficiency in three-dimensional soft agar culture was the number of visible colonies obtained relative to the number of initial cellular units. It may therefore be expressed as $\frac{\text{visible colonies obtained}}{\text{number of single cells seeded}} \times 100$. The frequency of colonies containing microcalculi formed in three-dimensional soft agar culture was also expressed by the following formula: $\frac{\text{number of colonies containing microliths}}{\text{50 colonies formed at 45 days of culture}} \times 100$.

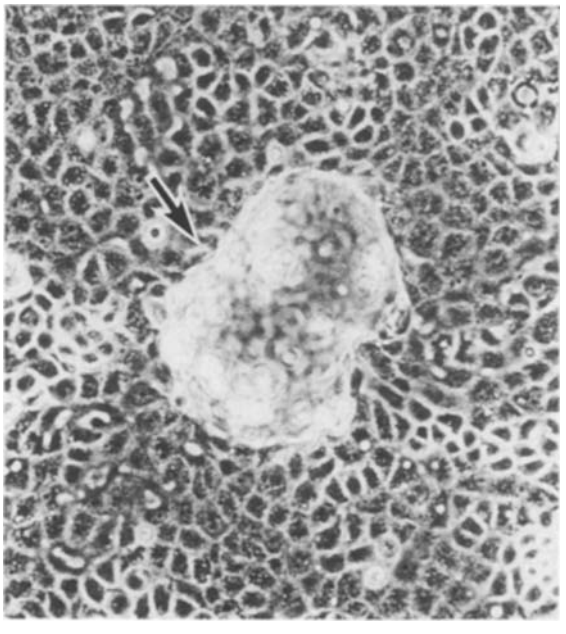

Fig. 1 A dome (*arrow*) which might have been formed by fusion of two domes in an MDCK cell sheet cultured at saturation density. Phase contrast photomicrograph, X600

Transmission electron microscopy

Cultured cells and colonies were fixed in 2% glutaraldehyde, postfixed in 1% osmium tetroxide for 1 h at 4°C, dehydrated in a graded alchohol series, and embedded in epoxy resin. Ultrathin sections were stained with uranyl acetate and lead citrate and examined with an H-700 transmission electron microscope (Hitachi Ltd.).

Scanning electron microscopy

Cultured cells and renal tissues were fixed in 2% glutaraldehyde, postfixed in 1% osmium tetroxide, dehydrated as described above, and dried by the critical point method using liquid CO_2 in a JEE-4B vacuum evaporator (Jeol Ltd.). Cell surfaces were coated with gold in a JFC-1100 ion coater (Jeol Ltd.) and observed with a JEOL JSM 35 scanning electron microscope (Hitachi Ltd.).

Examination of human renal stones

A tissue specimen was obtained from a nephrectomized kidney of a 49-year-old male patient with right renal lithiasis and hypercalcemia. The tissue was fixed in 10% formalin for 24 h and paraffin sections were stained with hematoxylin and eosin for histological examination to allow comparison with the localization of calcified crystals formed in cell cultures. Renal stones were also removed from a 51-year-old female with ureter lithiasis and hyperparathyroidism by electron-hydrolauric lithotriptor (EHL) flexible ureterorenoscopy [2] for morphological examinations of microrenal stones compared with those in cell cultures with a scanning electron microscope. The microliths were analyzed by micro-infrared spectroscopy (IR-700; Japan Spectroscopic Ltd., Tokyo, Japan).

X-ray and micro-infrared spectroscopic analysis

One micrometer sections from cultures and renal tissues embedded in resin were placed on carbon plates and examined with a Jeol200 CX electron microscope fitted with an Emax-3770 X-ray analyzer (Horiba Ltd.) to determine the composition of renal stones. Deparaffinized sections of colonies and cells were placed on carbon plates and subjected to a micro-infrared spectroscopic analysis with an IR-700 analyzer (Nihon Bunkou Ltd., Tokyo, Japan). We also calculated the Ca:P ratio in calcium phosphate stones by microscopic image analyzer (MOP Videoplan; Carl Zeiss Ltd.).

Results

Monolayer cell culture model of stone formation

Very small crystals were first detected as linear black dot spots after 21 days of culture. However, small linear crystals were laid down under an MDCK cell layer in contact with the plastic surface of the culture vessel after 30 days of culture (Fig. 2). These calcified crystals appeared to be tightly bound to the culture vessel, and this observation was confirmed by transmission electron microscopy at higher magnification (Fig. 3). After culture for 60 days, extensive aggregates were seen immediately beneath the cell sheet and in the domes (Fig. 4).

Fig. 2 Transmission electron microscopic appearance of calcified crystals (*) on plastic culture vessels under MDCK epithelial cells after 30 days of culture. *C* MDCK cells, *P* plastic culture vessel

Fig. 3 Higher resolution transmission electron microscopic appearance of calcified microcrystals (*) in the basal region of an MDCK cell after 30 days of culture. *C* MDCK cell

Fig. 4 Electron-dense calcified crystals (*arrows*) formed between MDCK confluent sheets (*CS*) including a dome (*D*) and the plastic culture vessel (*P*) in a 60-day culture. Scanning electron microscopy

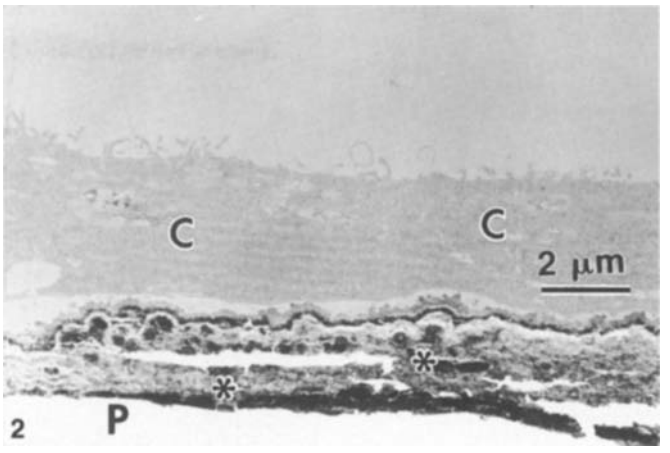

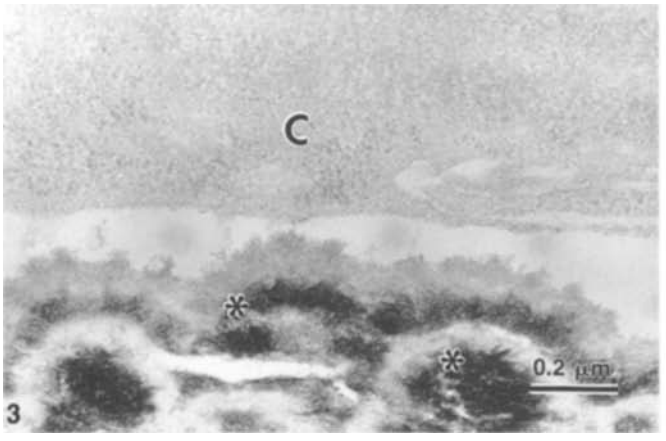

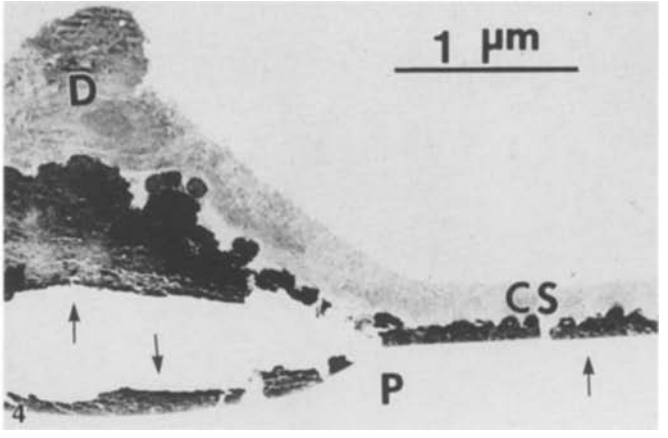

Three-dimensional soft agar culture model of stone formation

Very tiny crystals were first observed within pseudocysts at 28 days of culture. After about 8 weeks of culture, two types of colony, dark and clear, were also observed by phase contrast microscopy (Fig. 5A,B). The clear colonies were devoid of microliths (Fig. 5D), but small microliths were observed within pseudocysts formed by a single MDCK cell layer in dark colonies after 5 weeks of culture (Fig. 5C) by light microscopy. These colonies appeared to have a coralline or cauliflower-like shape (Fig. 5C). These microliths were closely similar in appearance to those observed in human specimens by scanning electron microscopy (Fig. 6A,B). The colony efficiency (the proportion of colonies formed to the total cells inoculated) in soft agar culture was 50.6 ± 2.6% ($P < 0.001$), and the frequency of colonies containing microcalculi was 55.6 ± 1.2% ($P < 0.001$).

Collagen gel culture model of stone formation

When a collagen gel bed was used, microcalcifications were first observed immediately beneath the single epithelial cell layer after 21 days of culture. These discrete and dense amorphous deposits increased in size and in number after 40–60 days of culture (Fig. 7A). These linear concretions were very similar in appearance to those in human urolithiasis (Fig. 7B). In the human specimens, microcrystals were also seen at or in the vicinity of the basal region of the tubular cells or in their vicinities (Fig. 7B).

X-ray and micro-infrared spectroscopic analysis

Electron microscopy confirmed the presence of electron-dense materials in all three types of cell culture. All of these electron-dense concretions were composed of calcium phosphate as demonstrated by X-ray and micro-infrared spectroscopy (Figs. 8, 9). Two types of calcium were detected by X-ray examination, calcium κ_α and κ_β. Both renal cell cultured and human renal concretions are also composed of calcium phosphate (Figs. 6B, 7B) with a Ca:P ratio of 2.7:1.

Discussion

In the present study we developed three systems of cell culture; monolayer, three-dimensional soft agar, and collagen gel culture, as models of renal stone formation; and undertook a morphological examination of the calcium phosphate renal microcalculi and calcifications that were formed in these models (Fig. 10).

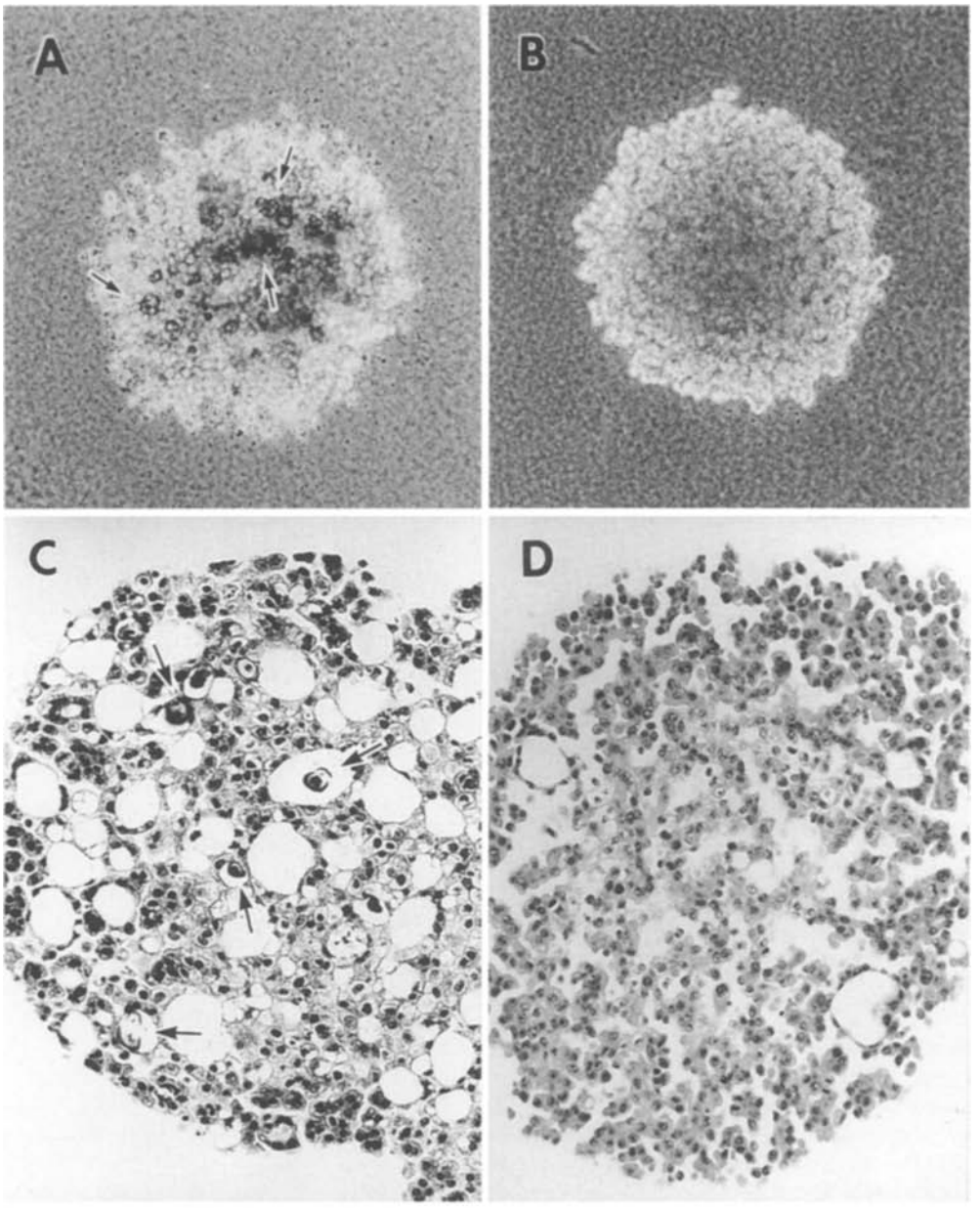

Fig. 5A-D A colony originating from a single MDCK cell after 60 days in three-dimensional soft agar culture. **A** A dark colony containing many microcalculi (*arrows*). **B** A clear colony free from microcalculi. **C, D** Dark and clear colonies, respectively, stained with hematoxylin and eosin. In the dark colony (**C**) miniature calculi (*arrows*) were found within pseudocysts formed by a single cell layer. A clear colony was free from calculi (**D**) **A, B** (phase contrast microscopy), X100; **C, D** (light microscopy), X200

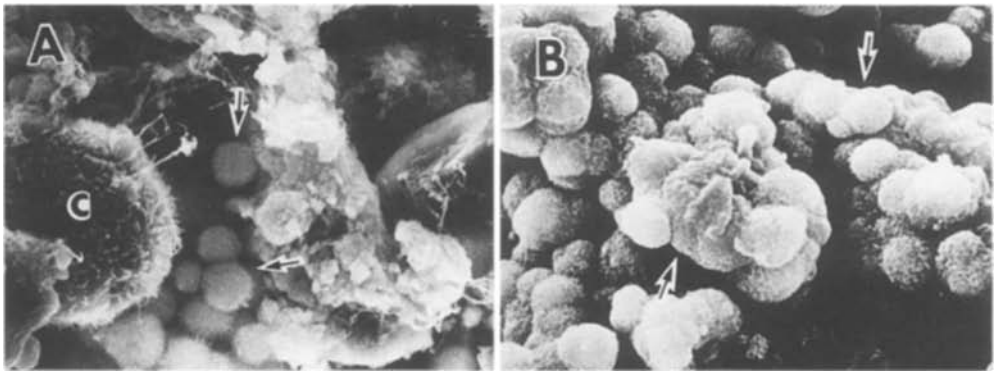

Fig. 6A, B Comparison of calculi formed in soft agar culture and those in a patient with renal calculous disease by scanning electron microscopy. **A** A cluster of small globular microcalculi with numerous fiber-like microprojections (*arrows*) adjacent to an MDCK cell (C) in a 50-day culture. **B** Microcalculi (*arrows*) formed in a patient with renal stone disease. **A** X4600, **B** X3000

Calcified microcrystals were located as discrete deposits, between the single cell layer and the surface of the culture dish, and in the collagen matrix. In three-dimensional soft agar cultures, microliths were detected within pseudocysts. These microliths had a lamellated and spherical structure by light microscopy. These linear-microcrystals and microliths were located corresponding to their location in human renal tubules; in

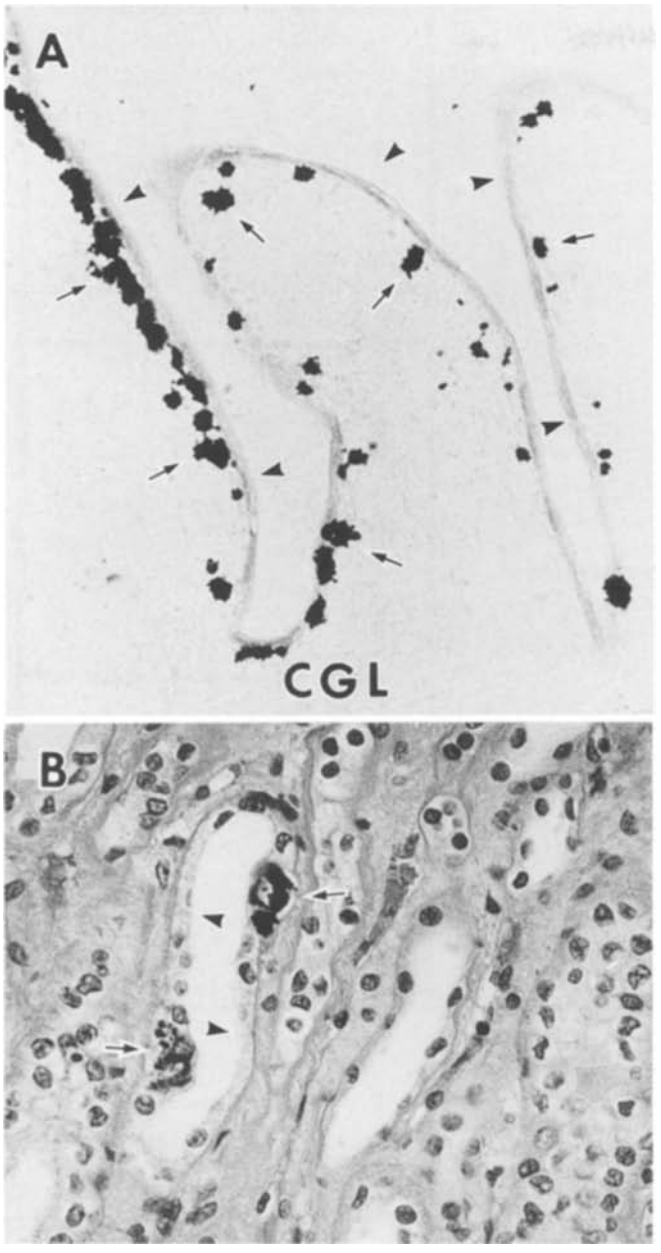

Fig. 7A, B Comparison of calcified deposits formed on collagen gel culture and in human renal tubules. **A** Discrete and dense deposits (*arrows*) immediately beneath the MDCK cell layer (*arrowheads*) in a 45-day culture on a collagen gel layer (*CGL*). **B** Microcrystals and large calcium concretions (*arrows*) apparently deposited between the basolateral site of the tubular epithelial cells and the underlying basement membrane in the interstitium in human renal lithiasis. **A, B** X275

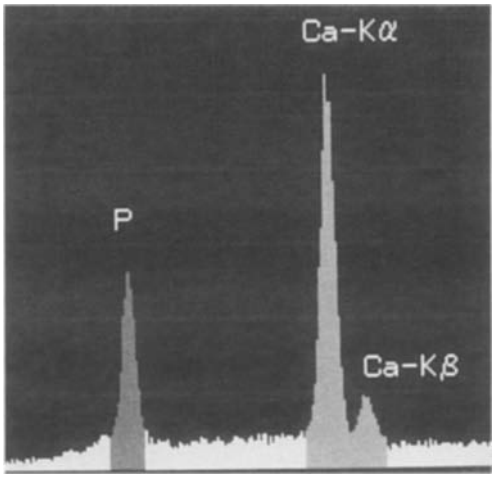

Fig. 8 X-Ray analysis of the composition of electron-dense deposits in the three types of cell culture. All the crystals were composed of calcium phosphate. There were two peaks of calcium, calcium κ_{α} and κ_{β}

the interstitum in the vicinity of renal epithelial cells. These findings indicate that the microconcretions originate in the interstitum facing the tubular epithelium, though the reason for this is still unknown.

Many small foci of calcification also appeared to be tightly bound to the culture vessel at an early stage of culture in the monolayer culture. These data may suggest that the deposits form due to active concentration of calcium and phosphate by the MDCK cells under the micro-environments where media are supersaturated and heteronucleation may occur. We did not, however, examine the pH, the buffer system, or Ca/P flux in this experiment. In addition, these findings suggest specific interactions between the extracellular matrix produced by the MDCK cells and some unknown factors in the microenvironment mediating crystallite formation [4, 11, 39, 40]. As the basal subcellular to pericellular calcium flux in confluent MDCK cells is 0.98 nmol/min/cm, calcium might be concentrated at the basal aspect of cell monolayers if the transported cations are not effectively removed [33, 34]. It is also conceivable that if the calcium ions transported across the tubular epithelial cells are not effectively removed, the local ionic concentration might rise beyond the saturation level and deposits might form, especially when the local pH is favorable for microcrystal formation.

The morphological appearance of calcified concretions differed from microliths at the light microscopic level, but ultrastructurally these two forms were morphologically similar. Furthermore, both these types of renal concretions were composed of calcium phosphate. Therefore, after they formed small clusters in renal tissues, some may develop into calcifications and others may develop into calculi depending on the sites, such as the intra- and extra-tissue environment of the kidney, at which they are generated in the renal tissue.

About 70–80% of renal stones are composed of calcium oxalate crystals with or without other components of calculi [6, 18, 28]. In patients with type I renal tubular acidosis, however, most renal crystals and calcified crystals are composed of calcium phosphate [35, 36]. Furthermore, the intrapapillary calculi chiefly consist of calcium phosphate in the usual renal stone disease [8, 18]. These concretions are generally observed at the basement membrane and in the interstitium of the renal collecting ducts and distal tubules, and a significantly higher mean calcium concentration gradient has been

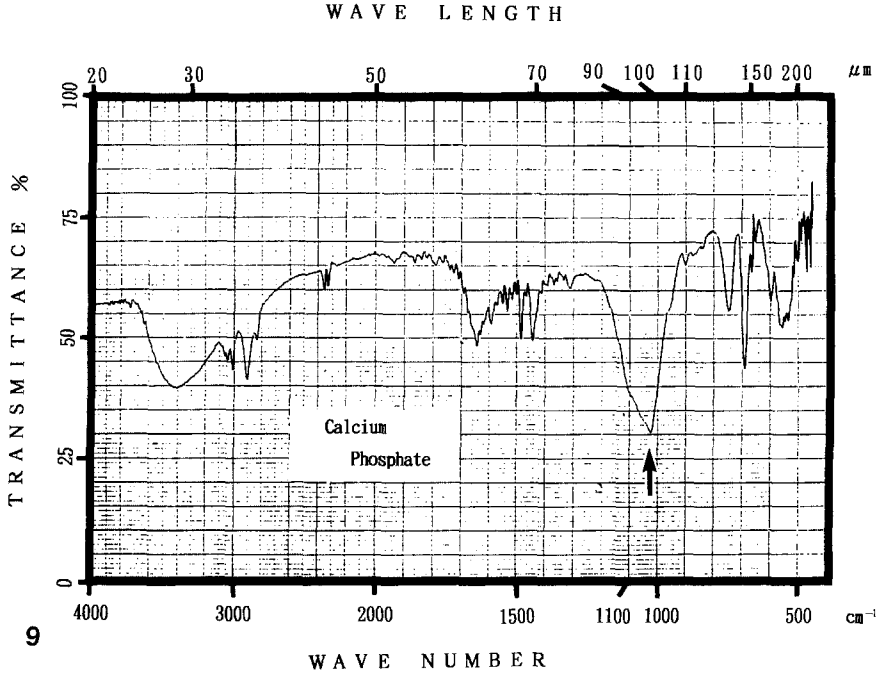

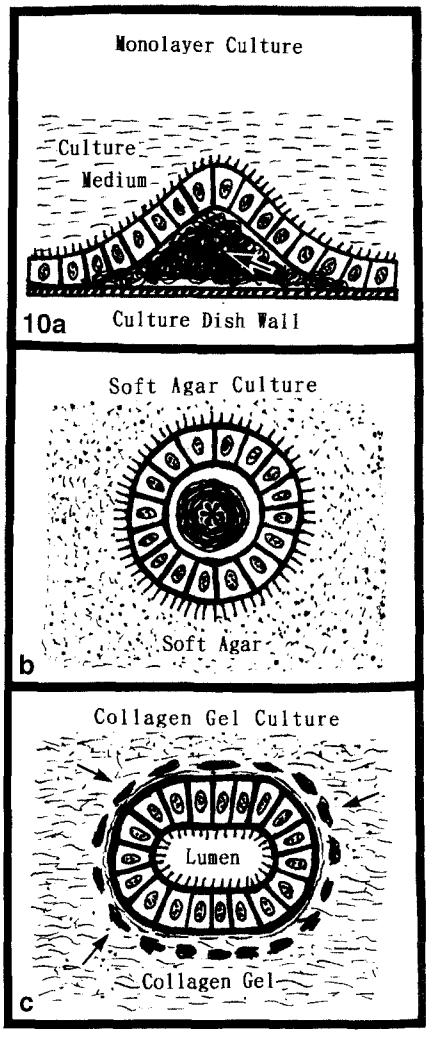

Fig. 9 Micro-infrared spectroscopic analysis of calcium phosphate in microcrystals formed in the three types of cell culture. *Arrow* shows the calcium phosphate peak

Fig. 10 Diagram of the localizations of miniature calculi and calcified crystals in the three cell culture models. *Arrows* calcified crystals, *star* microcalculus

detected in the medulla than in the cortex [16, 18, 19]. In this study, we used the MDCK cell line derived from renal distal tubular epithelium [28, 29] and showed that calcified crystals and miniature calculi composed of calcium phosphate were formed at the basal side (facing the impermeable culture dish or collagen gel matrix) of the monolayers. Therefore, our culture models may be a powerful new tool to study the pathogenesis of renal lithiasis and/or calcium phosphate stone formation in human and animals.

Small calcified crystals were morphologically first observed after culture at approximately 21–28 days. However, larger calculi could be observed after 30 days of culture. These findings strongly suggest that the deposits grow gradually, and are not an artifact of the long period of time used to maintain the culture. It is very difficult to determine the exact time of appearance of stones by histological examination of cell cultures or materials obtained from humans and experimental animals, because calculous deposits may be lost during fixation and sectioning of specimens [1]. In a previous study, we had observed calcium phosphate and calcium oxalate crystals by electron microscopy in human periosteal cells in monolayer cultures supplemented with ascorbic acid after 14 days of culture [39]. Thus these tiny concretions may be detected at an earlier stage in our culture systems by using contact radiography, which we shall pursue in the near future [45]. A morphological study of this kind may gives clues as to how and where renal microliths may develop, and our systems should be useful for analysis of the earliest events in renal stone formation.

Finally, many kinds of genetic changes may occur in cultured cells, especially during long-term culture. In the present study, three-dimensional soft agar cultures were found to contain two types of colony, one with renal microliths and the other with none. Comparison of mutants that do and do not generate renal stones may be useful to obtain further information on the mechanisms of calculogenesis. It would be of great interest to ascertain the complicated genetic factors associated with pathogenesis of renal stone formation including the predispositions to lithogenesis by using our culture models [5, 40].

Acknowledgements The authors thank Dr. Haruhiko Sugimura, Professor of the First Department of Pathology, Hamamatsu University School of Medicine, for helpful comments. They also thank Dr. Atsushige Sato (Second Department of Dental Technology, Faculty of Dentistry, School of Dental Surgery, Tokyo Medical and Dental University) for providing MDCK cells and

Dr. Yoshinori Muranaka, Center Laboratory for Ultrastructure Research, and Mr. Takaharu Kamo, First Department of Pathology, Hamamatsu University School of Medicine, for expert technical assistance in electron (Y.M.) and light (T.K.) microscopic studies. This work was supported by a Grant-in-Aid from the Ministry of Education, Science and Culture of Japan, and was presented in part at the 1993 Annual Meeting of the Japanese Tissue Culture Association, Tsukuba, Ibaragi.

References

1. Anderson CK (1979) The anatomical aetiology of renal lithiasis. In:Wickham J EA (ed) Urinary calculus disease. Churchill Livingstone, London, 40
2. Aso Y, Ohtawara Y, Fukuta K, Sudoko H, Nakano M, Ushiyama T, Ohta N, Suzuki K, Tajima A (1987) Operative fiberoptic nephroureteroscopy: Removal of upper ureteral and renal calculi. J Urol 137:629
3. Atmani F, Opalko FJ, Khan SR (1996) Association of urinary macromolecules with calcium oxalate crystals induced in vitro in normal human and rat urine. Urol Res 24:45
4. Barckhaus RH, Hohling HJ, Fromm I, Hirsch P, Reimer L (1991) Electron spectroscopic diffraction and imaging of the early and mature stages of calcium phosphate formation in the epiphyseal growth plate. J Microsc 162:155
5. Breuer WV, Mack E, Rothstein A (1988) Activation of K^+ and Cl^- channels by Ca^{2+} and cyclic AMP in dissociated kidney epithelial (MDCK) cells. Pflügers Arch 411:450
6. Coe FL, Parks JH (1988) Nephrolithiasis: Pathogenesis and treatment (2nd edn). Year Book Medical Publishers, Chicago, pl
7. Coe FL, Nakagawa Y, Asplin J, Parks JH (1994) Role of nephrocalcin in inhibition of calcium oxalate crystallization and nephrolithiasis. Miner Electrolyte Metab 20:378
8. Curhan GC, Curhan SG (1994) Dietary factors and kidney stone formation. Compr Ther 20:485
9. De Bruijn WC, Boeve ER, van Run PR, van Miert PP, de Water R, Romiji JC, Verkoelen CF, Cao LC, Schroder FH (1995) Etiology of calcium oxalate nephrolithiasis in rat. I. Can this be a model for human stone formation? Scanning Microsc 9:103
10. De Bruijn WC, Boeve ER, van Run PR, van Miert PP, de Water R, Romijn JC, Verkoelen CF, Cao LC, van 't Noordende JM, and Schrder FH (1995) Etiology of calcium oxalate nephrolithiasis in rats. II. The role of the papilla in stone formation. Scanning Microsc 9:115
11. De Vita MV, Zabetakis PM (1993) Laboratory investigation of renal stone disease. Clin Lab Med 13:225
12. Gaush CR, Hard WL, Smith TF (1966) Characterization of an established line of canine kidney cells (MDCK). Proc Soc Exp Biol Med 122:931
13. Goldfarb S (1994) Diet and nephrolithiasis. Annu Rev Med 45:235
14. Grases F, Sohnel O (1993) Mechanism of oxalocalcic renal calculi generation. Int Urol Nephrol 25:209
15. Grover PK, Ryall RL, Marshall VR (1992) Calcium oxalate crystallization in urine: role of urate and glycosaminoglycans. Kidney Int 41:149
16. Herzlinger DA, Eeston TG, Ojakian GK (1982) The MDCK epithelial cell line expresses a cell surface antigen of the kidney distal tubule. J Cell Biol 93:269
17. Hess B (1994) Tamm-Horsfall glycoprotein and calcium nephrolithiasis. Miner Electrolyte Metab 20:393
18. Hill GS (1992) Calcium and the kidney, nephrolithiasis, and hydronephrosis. In: Heptinstall RH (ed) Pathology of the kidney (4th edn). Little Brown, Boston, p 1563
19. Joos RW, Carr CW (1967) The binding of calcium in mixtures of phospholipids. Proc Soc Exp Biol Med 124:1268
20. Kennedy SM, Flanagan JL, Mills JW, Friedman PA (1989) Stimulation by parathyroid hormone of calcium absorption in confluent Madin-Darby canine kidney cells. J Cell Physiol 139:83
21. Khan SR (1995) Calcium oxalate crystal interaction with renal tubular epithelium, mechanism of crystal adhesion and its impact on stone development. Urol Res 23:71
22. Khan SR (1995) Experimental calcium oxalate nephrolithiasis and the formation of human urinary stones. Scanning Microsc 9:89
23. Lieske JC, Swift H, Martin T, Patterson B, Toback FG (1994) Renal epithelial cells rapidly bind and internalize calcium oxalate monohydrate crystals. Proc Natl Acad Sci USA 91:6987
24. Mandel N (1994) Crystal-membrane interaction in kidney stone disease. J Am Soc Nephrol 5 (Suppl 1):S37
25. Mandel N, Riese R (1991) Crystal-cell interactions: crystal binding to rat renal papillary tip collecting duct cells in culture. Am J Kidney Dis 17:402
26. Menon M (1993) A prospective study of dietary calcium and other nutrients and the risk of symptomatic kidney stones. J Urol 150:563
27. Pak CY (1994) Citrate and renal calculi: an update. Miner Electrolyte Metab 20:371
28. Peacock M, Robertson WG (1979) The biochemical aetiology of renal lithiasis. In:Wickham JEA (ed) Urinary calculus disease. Churchill Livingstone, London, p 69
29. Prien EL (1975) The riddle of Randall's plaques. J Urol 114: 500
30. Randall A (1936) A hypothesis for the origin of renal calculus. N Engl J Med 214:234
31. Randall A (1937) The origin and growth of renal calculi. Ann Surg 105:1009
32. Randall A (1940) Papillary pathology as a precursor of primary renal calculus. J Urol 44:580
33. Riese RJ, Riese JW, Kleinman JG, Wiessner JH, Mandel GS, Mandel NS (1988) Specificity in calcium oxalate adherence to papillary epithelial cells in culture. Am J Physiol 255:F1025
34. Robertson WG, Peacock M (1972) Calcium oxalate crystalluria and inhibitors of crystallization in recurrent renal stone-formers. Clin Sci 43:499
35. Robertson WG, Peacock M, Nordin BEC (1971) Calcium oxalate crystalluria and urine saturation in recurrent renal stone-formers. Clin Sci 40:365
36. Rosen S, Greenfeld Z, Bernheim J, Rathaus M, Podjarny E, Brezis M (1990) Hypercalcemic nephropathy: Chronic disease with predominant medullary inner stripe injury. Kidney Int 37:1067
37. Ryall RL (1993) The scientific basis of calcium oxalate urolithiasis. Predilection and precipitation, promotion and prescription. World J Urol 11:59
38. Scheinman SJ, Pook MA, Wooding C, Pang JT, Frymoyer PA, Thakker RV (1993) Mapping the gene causing X-linked recessive nephrolithiasis to Xp 11.22 by linkage studies. J Clin Invest 91:2351
39. Suzuki H, Naito Y (1991) An in vitro study on the characteristics of osteoblastic cells derived from human mandibular periosteum (in Japanese). J Jpn Stomatol Soc 40:89
40. Termine JD, Klineman HK, Whitson SW, Conn KM, McGarvey ML, Martin GR (1981) Osteonectin, a bone specific protein linking mineral to collagen. Cell 26:99
41. Torres VE, Wilson DM, Hattery RR, Segura JW (1993) Renal stone disease in autosomal dominant polycystic kidney disease. Am J Kidney Dis 22:513
42. Van Aswegen CH, Dirksen van Sckalckwyk JC, du Toit PJ (1992) The effect of calcium and magnesium ions on urinary urokinase and silicase activity. Urol Res 20:41
43. Verdier JM, Dussol B, Casanova P, Daudon M, Dupuy P, Berthezene P, Boistelle R, Berland Y, Dagorn JC (1993) Renal lithostathine: a new protein inhibitor of lithogenesis. Nephrologie 14:261
44. Wandzilak TR, Calo L, D'Amdre S, Borsatti A, Williams HE (1992) Oxalate transport in cultured porcine renal epithelial cells. Urol Res 20:341
45. Wang YH, Grenabo L, Hedelin H, McLean RJ, Nickel JC, Pettersson S (1993) Citrate and urease-induced crystallization in synthetic and human urine. Urol Res 21:109